ACS Catalysis

Research Article

pubs.acs.org/acscatalysis

Remote Activation of Chemical Bonds in Heterogeneous Catalysis

Anton M. H. Rasmussen, Michael N. Groves, and Bjørk Hammer*

iNANO and Department of Physics and Astronomy, Aarhus University, 8000 Aarhus C, Denmark

Supporting Information

ABSTRACT: A catalyst is generally considered to act locally at the reaction site. For heterogeneous catalysis, this concept should be extended to include the influence of the surface on the nonreacting regions of the reactants because this can lead to more favorable reaction paths. In this work, density functional theory is used to examine how a Pt(111) surface hydrogenates the ketone 2,2,2-trifluoroacetophenone (TFAP). It is revealed that the platinum activates TFAP through an interaction with a part of the molecule remote from the reaction while simultaneously mediating the hydrogenation of the carbonyl. The remotely activated state is formed through double bond migration enabled by the malleable electronic structures of the chemisorbed phenyl ring and platinum surface. By forming an enol, the TFAP carbonyl is able to decoordinate from the Pt surface reducing steric and electronic interference that inhibits hydrogenation. This result illustrates the necessity of considering catalyst interactions with molecular parts remote from the reaction site with processes involving a heterogeneous catalyst.

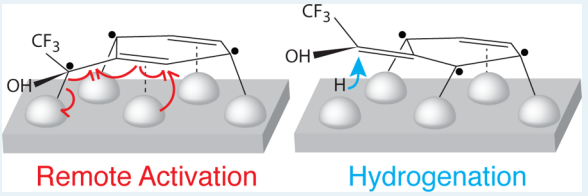

KEYWORDS: *heterogeneous catalyst, density functional theory, asymmetric hydrogenation, adsorption effect, remote catalysis, double-bond migration, α-fluoroketone*

1. INTRODUCTION

The role of a catalyst in a reaction is to provide a lower-energy pathway from the reactants to the products. This is typically viewed as a localized process in which the catalyst acts at the reaction site to activate intermediates and facilitate the reaction. For instance, in homogeneous catalysis, the metal center of an organometallic complex is considered the principle actor in catalyzing a given mechanism, and this has proven to be an effective model in describing a wide variety of reactions. This includes the Heck reaction,[1,2] the Suzuki reaction,[3,4] and the Grubbs catalyst,[5,6] which all led to Nobel prizes for their namesakes. Reactions that involve double bond migration have also been described as being mediated by an organometallic compound principally using the metal center.[7] On the other hand, reactions without direct metal coordination are also known; for example, hydrogen transfer between alcohols and ketones,[8] and methods involving metal coordination to molecule parts remote from bonds to be cleaved also exist.[9]

Turning to heterogeneous catalysis, the level of complexity used to describe a catalytic metal surface varies depending on the amount of detail required to explain its involvement in the reaction. At one end of the spectrum, no precise atomic resolution is required to explain the surface−reactant interaction.[10−12] In this case, the reaction properties discussed are macroscopic in scope. This includes predicting and measuring trends in reaction rates[13,14] or catalyst stability under reaction conditions.[15,16] At the other end of the spectrum, it is necessary to discuss the interplay of individual atoms and their critical role required for the reaction to proceed. This includes cases in which geometrical factors are important, such as near corners, kinks, and steps,[17−21] or when discussing the ensemble effect.[22−24] In many of these systems, the catalyst is described as acting at a single part of the reactant. To the authors' knowledge, the possibility that the surface can simultaneously act on a remote part of a reactant to stimulate the progress of the reaction is not discussed in the literature on surface catalysis.

The present work illustrates that the interaction among all parts of the reactants and the metal should be examined when describing reactions on surfaces. Using density functional theory (DFT), we investigate the hydrogenation mechanism of the ketone 2,2,2-trifluoroacetophenone (TFAP) over Pt(111) to the corresponding unsaturated alcohol. TFAP is a commonly studied reactant in asymmetric hydrogenation over modified heterogeneous catalysts. Thus, it is important to investigate its hydrogenation in detail.[25−32] Supported platinum is a well-known heterogeneous catalyst for the selective hydrogenation of ketones into unsaturated alcohols, and the metal surface is known to provide atomic hydrogen by splitting the gas into individual atoms. The details of the activation of the ketone carbonyl are not well-known. We find that the preferred reaction path for TFAP involves partial decoordination of the substrate facilitated by an interaction between the metal and the nonreacting phenyl part of the molecule. In the gas phase, the electronic structure used to describe this transition would be similar to that of the benzyl radical; however, the conjugated nature of the phenyl ring disappears upon adsorption onto the surface. This correlates with a more substantial involvement of the platinum with the remote phenyl moiety to activate the

Received: October 2, 2013
Revised: February 10, 2014
Published: March 3, 2014

   dx.doi.org/10.1021/cs400875k | ACS Catal. 2014, 4, 1182−1188

TFAP carbonyl, highlighting the catalyst's ability to perform multiple functions on the same molecule.

2. COMPUTATIONAL METHODS

DFT calculations were carried out for coadsorbed TFAP and hydrogen on Pt(111) using the ASE[33] and GPAW[34,35] 0.9 open source software codes. For this work, the GPAW 0.8 projector augmented wave (PAW) setups are used. Electron−electron interactions were treated with the optB88-vdW[36] exchange-correlation functional to include the subtle dispersion-related interactions among the substrate, the hydrogen atoms, and the platinum surface. For example, the optB88-vdW functional can predict the experimental binding energy for the difficult to quantify benzene/platinum interaction.[37] A convincing description of the adsorption of benzene on platinum is fundamental to the extended catalyst concept presented in this work. The platinum surface was modeled with a four-layer slab that is periodic in the x and y directions. Each layer is composed of 16 Pt atoms, and the bottom layer was fixed. The Brillouin zone is sampled using a 2×2 grid of **k**-points. The x/y components of the cell that were used for all calculations are 11.37 Å/9.85 Å and were defined by the 4.02 Å optB88-vdW lattice constant for Pt. A cell height of 24.04 Å was used in the z direction. This choice of z direction cell size provided a 6 Å space both above the top of the molecules adsorbed onto the slab and below the bottom layer of the slab. The GPAW software resolves the electronic density and orbitals on a real space grid. In this case, a grid spacing of 0.1777 Å/0.1758 Å/0.1768 Å was used for the $x/y/z$ axis. Geometries were relaxed until forces were below 0.01 eV/Å on each atom. To find transition paths and barriers, we used the climbing image nudged elastic band method.[38] Saddle points were relaxed to below 0.01 eV/Å. Vibrational frequencies were calculated for all saddle points and minima using the harmonic approximation. This was to confirm the type of stationary point calculated as well as to determine their zero-point energy (ZPE) correction, which can be significant when adding hydrogen atoms from the surface to a molecule.[39] These modes were determined by constructing the Hessian matrix through finite differencing of the forces at ±0.01 Å in the $\pm x$, $\pm y$, $\pm z$ direction.[40] Only adsorbates were included in the atomic displacements. All energies quoted in this work include the ZPE correction. Supporting Information Table S1 includes the noncorrected energies. Atomic coordinates and absolute energies from all relaxations can also be found in the Supporting Information.

3. RESULTS

In general, TFAP may adsorb in numerous ways. Here, we concentrate on the previously determined low-energy ketone geometry[41,42] shown in the bottom left panel of Figure 1. This geometry has simultaneous coordination to the metal with both phenyl and carbonyl groups.

Initially, to probe the stability of TFAP at different stages of hydrogenation, we move one or two hydrogen atoms from the surface to the carbonyl. Resulting optimized geometries are displayed in Figure 1. The addition of one hydrogen reveals that the semihydrogenated hydroxy intermediate is the surface species with the overall lowest energy. The potential energy change for this step (including ZPE) is −0.18 eV relative to the adsorbed ketone, indicating that in the presence of adsorbed hydrogen, this semihydrogenated intermediate is strongly favored thermodynamically over the separated reactants. The

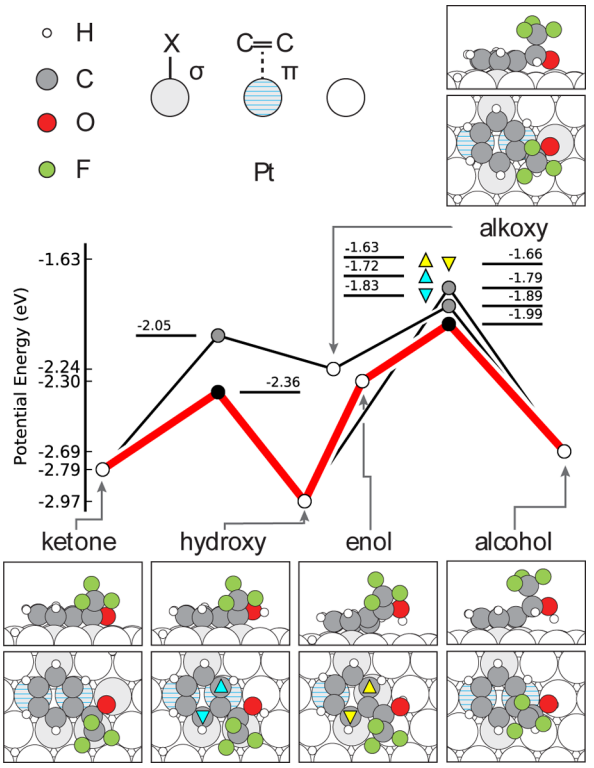

Figure 1. Energy diagram of all the investigated routes of hydrogenation. Solid symbols represent transition states; open symbols denote minima. The reference energy is calculated from the separated components: a four-layer Pt(111) slab, an isolated TFAP molecule, and isolated H_2. Zero-point energy corrections have been applied. Insets: Geometries of adsorbed TFAP at different stages of hydrogenation. In all cases, an appropriate number of hydrogen atoms are on the Pt surface (2 for the ketone, 1 for the three intermediates). The triangles (Δ/∇) represent the transition state energy for the addition of a hydrogen atom to the bridged and apical carbons adjacent to the ipso carbon. They are colored blue and yellow to indicate if this addition was done from the hydroxy or enol state, respectively. In the case of the ketone, hydroxy, and alkoxy geometries, there are platinum atoms inserted into the carbonyl group bonds.

alternative addition of the same hydrogen to the carbonyl carbon forms a higher-energy alkoxy intermediate. Completion of the hydrogenation reaction and formation of the alcohol results in a 0.28 eV increase in energy compared with the hydroxy intermediate.

Several reaction pathways were calculated, and their energy profiles are also shown in Figure 1. The preferred route is highlighted in red, and will be discussed first. The reaction proceeds by stepwise addition of atomic hydrogen. From the stability of the hydroxy intermediate, it may be expected that hydrogenating the carbonyl oxygen first is preferred over the adjacent (benzylic) carbon. This is, indeed, the case, and the ketone-to-hydroxy activation energy is 0.43 eV. Thus, hydrogenating the oxygen is a fast process at room temperature. The addition takes place from a precursor in which the hydrogen atom is adsorbed atop a Pt adjacent to the chemisorbed oxygen. From this position, the hydrogen atom approaches the lone pair of oxygens; hence, the electronic system may easily change from Pt−H···O−Pt to Pt···H−O···Pt. In the resulting hydroxy intermediate, the benzylic carbon is σ-bonded to a Pt to saturate its valence shell.

dx.doi.org/10.1021/cs400875k | ACS Catal. 2014, 4, 1182−1188

To complete the hydrogenation reaction, the benzylic carbon is now hydrogenated. However, prior to accepting the second hydrogen, the reacting group lifts away from the surface into an enol intermediate. This state is possible only through simultaneous double bond migration and modification of the phenyl-platinum interaction. This will be described in the next paragraph. The hydrogen addition proceeds by H moving on top the Pt that previously bonded to C, followed by the formation of the C−H bond. The total barrier to form the enol and add the hydrogen is 0.98 eV. Despite this apparently high barrier, it is the investigated path of overall lowest energy. This value for the activation energy is twice what was determined for the hydrogenation of acetophenone[43] but is consistent with the values found for the hydrogenation of other carbonyls.[44−46]

Now we return to the enol intermediate, which will be analyzed in terms of interatomic distances to infer intramolecular bond strength. During the decoordination from hydroxy to enol, the benzylic carbon releases its bond to Pt, shifting from tetrahedral to trigonal planar coordination. As such, a rearrangement of bond lengths is expected within the molecule. Figure 2 shows selected C−C bond lengths along with ball and stick illustrations of the hydroxy, enol, and alcohol structures of TFAP on Pt(111).

The C−C bond between the benzylic carbon and the phenyl ring is shown in yellow in Figure 2. It significantly decreases from 1.51 to 1.39 Å as TFAP transitions between the hydroxy and enol intermediates. This implies that a much stronger bond is formed between these two carbon atoms as the side group lifts away from the surface, compensating for the lost C−Pt bond. As hydrogen subsequently attacks the decoordinated benzylic carbon, completing the hydrogenation reaction, this stronger bond weakens as it elongates to 1.54 Å.

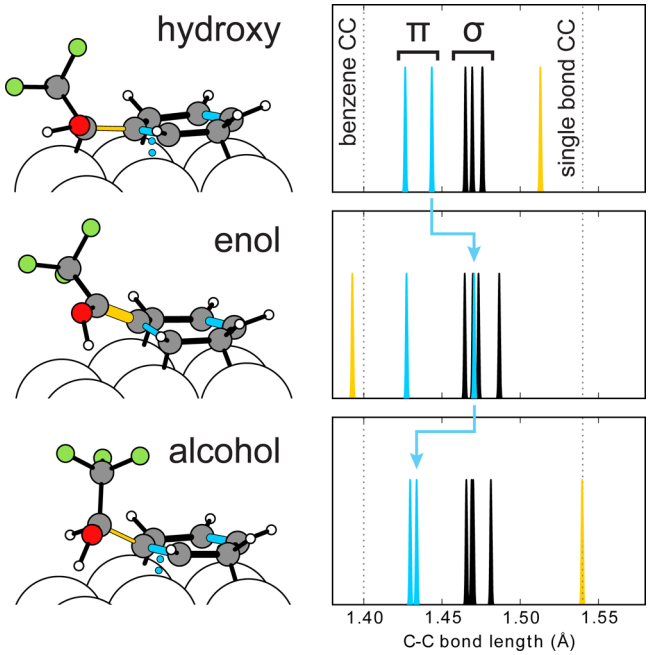

Figure 2. Analysis of carbon−carbon bond lengths (right) for geometries (left) at different stages of reaction. The two carbon−carbon bonds involved in bond migration are marked in yellow (phenyl-side group) and azure blue (internal phenyl). The hydroxy intermediate (top) has benzene-like phenyl−Pt bonding as well as a benzylic C−Pt σ bond. In the enol intermediate (middle), that σ bond is broken, a phenyl double bond has migrated to the side group forming an enol, and the phenyl now bonds to Pt with an additional σ bond. Finally, the alcohol (bottom) recovers the benzene-like phenyl-Pt coordination of two π bonds and two σ bonds.

A critical part of the favored pathway is how the bond lengths within the phenyl ring also change during the reaction. Initially, when the phenyl ring adsorbs onto the platinum surface, its conjugated character is lost due to the lower symmetry of the adsorption site. This interaction can be understood in terms of a donation−backdonation interaction between the benzene molecular orbitals and metal d states. For the TFAP hydrogenation reaction, it is instructive to employ a complementary view that describes a local interaction using distinct submolecular bonding mechanisms.[47] Under this scheme, two C−C double bonds are partly localized, forming π-bonds that interact with the underlying Pt atoms. These bonds are slightly elongated to 1.43 and 1.44 Å from their gas phase values of 1.40 and 1.41 Å. This bonding can be compared with that of π-bonded ethylene that has a 1.41 Å C−C distance.[48] The four remaining C−C bonds connect to the two apical carbons that are σ-bonded to individual Pt atoms. Each of these four bonds straddles two Pt atoms and is further elongated to 1.47−1.48 Å, reflecting a rehybridization that shows increased sp^3 character induced by the Pt σ bonds.

We denote these two types of phenyl C−C bonds[49] as π and σ. To illustrate the distinction between them, the localized π-bonded C−C interactions are highlighted in blue in Figure 2. In the hydroxy state, these C−C bond lengths are distinct from those of the σ type C−C bonds, which are illustrated in black. The slight length difference between the two π bonds can be explained by the side group's being associated with the longer double-bonded carbon pair. As the side group decoordinates from the surface to form the enol, that longer double bond elongates further and falls into the range of the four σ bonds as illustrated with the blue arrow. Finally, when the alcohol is formed, this bond contracts to match more closely its original length. The concurrent changes of the side group C−C bond length and phenyl π-bond lengths indicate that a double bond migrates from the ring to the side group and back during the hydroxy−enol−alcohol reaction steps.

When the double bond is outside the ring, the carbon atom in the ring that loses its double bond will be undercoordinated unless it forms another bond. The interatomic distance between this carbon, and its underlying platinum atom decreases from 2.20 to 2.15 Å, indicating that a stronger interaction occurs between the two and as a result adequately stabilizes the carbon atom. Thus, the malleable electronic structure of the adsorbed phenyl ring and the platinum surface allows for the enol intermediate to exist and makes the low-energy pathway possible. As a result, the surface has two key functions: it catalyzes the hydrogenation at the carbonyl site while simultaneously activating the TFAP molecule through the phenyl ring.

The electronic rearrangement calculated in TFAP for the hydroxy-to-enol transition is akin to what can be observed with the benzyl radical. In the gas phase, the spin density of the unpaired electron of the benzyl radical on the exomethylene is ∼0.7−0.8. The remainder is shared over the ortho and para positions of the phenyl ring.[50] This radical has been shown to have five resonant structures that contribute almost equally to the molecular geometry,[51] where all the C−C bond lengths range from 1.391 to 1.428 Å.[52] Thus, in the gas phase, it is not surprising that the unpaired electron can be seen to migrate

dx.doi.org/10.1021/cs400875k | ACS Catal. 2014, 4, 1182−1188

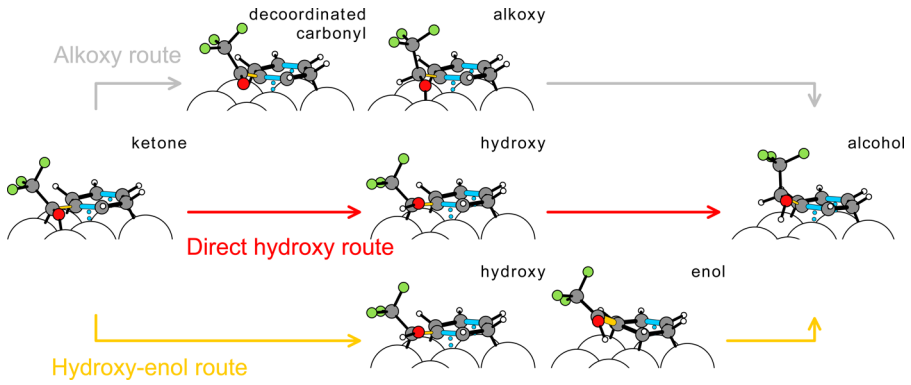

Figure 3. Reaction mechanisms for the three paths considered.

from the benzylic carbon to the ortho position of the phenyl ring for the hydroxy-to-enol transition calculated for TFAP.

The analogy with the benzyl radical ends when TFAP is adsorbed onto the surface, resulting in the previously discussed changes to its electronic structure. One consequence is the energetic penalty required for the platinum surface to stabilize TFAP from the ortho position of the phenyl ring (enol intermediate) instead of the benzylic carbon (hydroxy intermediate). In the gas phase, both of these intermediates would be simultaneously accessible as a superposition of both states. The interaction of the Pt surface has collapsed the delocalized system into distinct states with unique energies. Given that adsorbed intermediates can have different electronic structures from their gas phase analogues, mechanistic comparisons between both phases should be applied with caution.

To challenge the remotely activated pathway, conventional reaction paths need also be considered. In this case, hydrogenation involves the addition of two hydrogen atoms. This may happen in either a stepwise or a simultaneous fashion. Stepwise hydrogenation of carbonyls over a metal catalyst can proceed through two different surface intermediates: either by hydrogenating the carbonyl carbon, which forms a Pt−O bonded alkoxy; or by attacking the carbonyl oxygen first, which leads to a Pt−C bonded hydroxy. For example, the hydrogenation of aldehydes and ketones over Ru(0001) has been calculated to prefer reaction paths through very stable alkoxy intermediates, albeit facing high barriers in the ensuing reaction step.[53] Conversely, hydrogenation of the carbonyl of acrolein over Pt(111) has been shown to proceed through a hydroxy intermediate.[46,54]

Two alternative stepwise pathways were thus considered. Direct addition of hydrogen to the hydroxy intermediate was calculated as well as a path that involves hydrogenating the benzylic carbon first, leading to an alkoxy intermediate. Schematics of all three calculated pathways are presented in Figure 3, and the two additional energy landscapes are included in Figure 1. For the hydrogenation of TFAP, no simultaneous reaction paths were found. Attempts in that direction lead to the already considered hydroxy−enol mechanism.

First, the direct hydrogenation route without prior decoordination of the hydroxy intermediate will be discussed. Although the formation of the hydroxy moiety had a low barrier, it is strongly bound to platinum through a Pt−C σ bond. Thus, for the second hydrogenation, a direct reaction mechanism involving a three-center Pt−H−C transition state is found to have the highest overall transition state energy of the three paths considered (E = −1.79 eV, corresponding to an activation energy of 1.18 eV). This mechanism involves H climbing the Pt to which C is still bound, similar to what is found for hydrogenation of σ-bonded carbons of benzene/Pt(111)[55] and ethylene/Pd(111)[56] systems. It is perhaps no surprise that this scenario produces a high reaction barrier because the benzylic carbon atom is sp^3-hybridized, with each molecular orbital already bonded to another species. On the contrary, in the favored hydroxy−enol mechanism, the benzylic carbon rehybridizes to an sp^2 configuration and, thus, has a p_z orbital susceptible to hydrogenation.

In the second alternative route, the first hydrogen is added to the carbon to form an alkoxy species. This state is found to be disfavored by 0.73 eV compared with the hydroxy species. The hydrogenation is not direct, but is preceded by decoordination and recovery of the C═O double bond. Hydrogenation then occurs as the H climbs on top of the Pt to which the carbon was previously bonded. Finalizing this route, the addition of hydrogen to the oxygen atom is facile relative to the alkoxy state with a barrier of 0.35 eV. However, due to the high energy of the alkoxy intermediate, the transition state energy is 1.08 eV above the hydroxy state, and as a result, this route is only the second most favorable.

It is interesting that we find decoordination prior to carbon hydrogenation in both the alkoxy and hydroxy−enol routes. The preference for decoordination in both hydrogen-to-carbon addition steps illustrates that the benzylic carbon is not easily hydrogenated when σ-bonded to Pt. The idea of decoordination prior to H attack has previously been investigated; its importance is dependent on the chemical species involved.[57] Here, we find that the decoordination involves recovery of the reacting C═O double bond in the alkoxy path and formation of a C═C bond in the hydroxy-enol route. For the alkoxy case, direct reactions involve the decoordinated mechanism. In the other case, the direct hydroxy path is energetically disfavored, despite the significant bond rearrangements involved in the decoordination calculated in the hydroxy−enol route.

In addition to the two alternative routes, hydrogenation of both ortho carbon atoms from the hydroxy and enol states was performed. This was to ascertain the likelihood of hydrogenating the phenyl ring instead when the complex is in its most stable configuration as well the proposed key intermediate for the most favorable path from ketone to unsatruated alcohol. The saddle points for all four side reactions are included in Figure 1 using the Δ and ∇ symbols to represent the addition of a hydrogen atom to the bridged and apical carbons adjacent to the ipso carbon, respectively. Blue symbols denote when the

dx.doi.org/10.1021/cs400875k | ACS Catal. 2014, 4, 1182−1188

hydrogen is added to the hydroxy, and yellow ones are for when the enol is the initial case. One important result is that the hydrogenation of both ortho carbon atoms of the enol are more costly than for the hydroxy. This implies that the availability of the enol intermediate decreases the possibility of alternatively hydrogenating the ring instead of the carbonyl for a hydrogen atom in close proximity to the carbonyl. An additional consequence of the bond rearrangement necessary to form the enol intermediate results in a higher selectivity toward forming the alcohol.

All of these reaction paths are calculated under extremely low hydrogen conditions. Experimentally, as the hydrogen pressure increases, so does the reaction rate for the hydrogenation of TFAP.[59] In addition, computational studies have also shown that as the concentration of hydrogen increases on a Pt nanoparticle the energy of adsorption per adatom decreases until it is no longer favorable to add another adatom to the surface.[60] This coincides with a decrease in the activation energy required to desorb two adatoms and form H_2.[61] Given these results, it is presumed that as the surface reaches a high surface coverage of extra hydrogen adatoms, this would result in a reduction in the calculated activation energy for the hydrogenation of TFAP. This reduction would continue as the H adatom concentration is increased until it becomes more favorable for the adatoms to desorb instead.

4. DISCUSSION

The presented reaction pathway for TFAP has at least three implications on work being carried out in the context of stereoselective TFAP hydrogenation. First, surface science experiments reveal that the alcohol of TFAP adsorbed on Pt(111) and annealed to room temperature produces vibrational spectra and STM motifs identical to those of TFAP.[58] This observation was interpreted as conversion from alcohol to ketone, and the present calculations confirm that the adsorbed ketone is energetically preferred over the alcohol. However, the experiments indicate a change in the observed spectrum upon annealing the adsorbed alcohol, and in combination with the calculated low energy of the hydroxy intermediate, this suggests that the hydroxy species could be the source of the common vibrational spectrum. Second, in the Orito reaction, 1:1 complexes between adsorbed reactants and modifiers are believed to play a crucial role in the asymmetric discrimination. It has recently been investigated that the product alcohol of TFAP also binds strongly to the modifier and how this interaction critically affects the possible reaction mechanisms.[62] Also in this case, we propose that the semihydrogenated intermediates should be considered. Finally, a more speculative application of the remote activation in TFAP could offer an explanation to an outstanding question in the Orito reaction. The introduction of small amounts of modifier can greatly accelerate the hydrogenation of the prototypical reactant ethyl pyruvate.[63] In contrast, only a modest acceleration or even deceleration is observed in the case of TFAP[64,65] and other α-phenyl ketones.[66−68] This lack of modifier acceleration has been interpreted in terms of TFAP dimers in which the hydrogenation would be already accelerated before introduction of the modifier.[26] The activating effect of dimers cannot be excluded on the basis of the present results, but the hydroxy−enol reaction mechanism suggests that already, the TFAP monomer is intrinsically activated by the phenyl ring.

For other substrates,[69] such as methyl pyruvate, the hydrogenation reaction proceeds through an enol intermediate that is possible through keto−enol tautomerization,[70] but because of its fluorination, enolization is usually not considered relevant for TFAP.[58] The adsorption of the phenyl ring and the accompanying possibility of bond migration provides an alternative enolization route. Even the two paths not involving an enol state show subtle intramolecular changes similar to what was calculated in the enol route, as shown in Supporting Information Figure S1. The identified possibility that a catalyst surface can activate a reaction by interacting with a remote nonreacting part of the molecule illustrates that the local coordination of reacting species may not entirely describe their reactivity.

The active involvement of a phenyl ring adjacent to a ketone being hydrogenated may be relevant to some additional experimental observations. As an example, we apply our findings to the hydrogenation of 1-phenyl-1,2-propanedione (PPD). This diketone, illustrated in Figure 4, can be readily

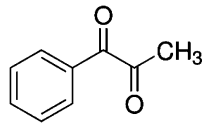

Figure 4. Illustration of 1-phenyl-1,2-propanedione.

hydrogenated on supported platinum[71] or palladium[72] to form 1-hydroxy-1-phenyl-2-propanone. Importantly, the ketone group adjacent to the phenyl ring is preferentially hydrogenated over the other ketone group. The rationale for this regioselectivity proposed by Nieminen et al. has two parts:[73] First, the most favorable configuration of PPD on platinum has both the phenyl ring and the adjacent ketone group adsorbed onto the metal. Geometries with the other ketone group chemisorbed are less stable. Second, it is assumed that coordinating the carbonyl to the surface activates it for hydrogenation;[74] therefore, a larger proportion of the ketone groups adjacent to the phenyl will be activated leading to preferential hydrogenation of this carbonyl. The present results for TFAP are consistent with this rationale; however, we additionally propose that the phenyl ring adsorbed to the metal surface activates the α-carbonyl and provides a low-energy pathway that the β-carbonyl does not have access to.

5. CONCLUSIONS

By examining the hydrogenation of TFAP on Pt(111), it has been calculated that the lowest energy route involves the surface to activate the molecule in two locations. In the first hydrogenation step, metal coordination activates the carbonyl directly. In the second and rate determining step, the catalyst surface interacts with the remote phenyl ring to activate the benzylic carbon via decoordination into an otherwise inaccessible enol state. The partly decoordinated enol lets the platinum atoms local to the benzylic carbon facilitate the hydrogenation reaction with the lowest reaction barrier. The decoordination of the hydroxy intermediate is found to be facilitated by double bond migration from the adsorbed phenyl to the side group. This double bond migration is possible due to the malleable electron structure of the phenyl/Pt system that maintains the filled valence shell of the carbon left unsatisfied by the migration.

Finally, although this work examines only TFAP and similar molecules, it is not expected that such multiple reaction site behavior shown by the platinum surface is limited to the

dx.doi.org/10.1021/cs400875k | ACS Catal. 2014, 4, 1182−1188

studied family of molecules. Instead, just as one must consider the reactivity at different sites on a heterogeneous catalyst, it appears necessary to also take into account the full set of molecule-surface interactions, including those of nonreacting remote moieties.

■ ASSOCIATED CONTENT

Supporting Information

An additional figure (Figure S1) and table (Table S1). Atomic positions of all relaxed structures and transition states with their calculated absolute energy. This material is available free of charge via the Internet at http://pubs.acs.org/.

■ AUTHOR INFORMATION

Corresponding Author

*E-mail: hammer@phys.au.dk.

Notes

The authors declare no competing financial interest.

■ ACKNOWLEDGMENTS

This work was supported by the Lundbeck Foundation, The Danish Council for Independent Research, and the Danish Center for Scientific Computing. The authors also thank Guillaume Goubert and Peter H. McBreen for informative discussions during the preparation of the manuscript.

■ REFERENCES

(1) Beletskaya, I. P.; Cheprakov, A. V. *Chem. Rev.* **2000**, *100*, 3009−3066.
(2) Dounay, A. B.; Overman, L. E. *Chem. Rev.* **2003**, *103*, 2945−2963.
(3) Miyaura, N.; Yamada, K.; Suzuki, A. *Tetrahedron Lett.* **1979**, *36*, 3437−3440.
(4) Phan, N. T. S.; Sluys, M. V. D.; Jones, C. W. *Adv. Synth. Catal.* **2006**, *348*, 609−679.
(5) Schwab, P.; France, M. B.; Ziller, J. W.; Grubbs, R. H. *Angew. Chem., Int. Ed.* **1995**, *34*, 2039−2041.
(6) Vougioukalakis, G. C.; Grubbs, R. H. *Chem. Rev.* **2010**, *110*, 1746−1787.
(7) Kuznik, N.; Krompiec, S. *Coord. Chem. Rev.* **2007**, *251*, 222−233.
(8) Yamakawa, M.; Ito, H.; Noyori, R. *J. Am. Chem. Soc.* **2000**, *122*, 1466−1478.
(9) Oh, M.; Yu, K.; Li, H.; Watson, E. J.; Carpenter, G. B.; Sweigart, D. A. *Adv. Synth. Catal.* **2003**, *345*, 1053−1060.
(10) Cremer, P. S.; Su, X.; Shen, Y. R.; Somorjai, G. A. *J. Am. Chem. Soc.* **1996**, *118*, 2942−2949.
(11) Taylor, C. D.; Wasileski, S. A.; Filhol, J.-S.; Neurock, M. *Phys. Rev. B* **2006**, *73*, 165402.
(12) Kanuru, V. K.; Kyriakou, G.; Beaumont, S. K.; Papageorgiou, A. C.; Watson, D. J.; Lambert, R. M. *J. Am. Chem. Soc.* **2010**, *132*, 8081−8086.
(13) Nørskov, J. K.; Rossmeisl, J.; Logadottir, A.; Lindqvist, L.; Kitchin, J. R.; Bligaard, T.; Jónsson, H. *J. Phys. Chem. B* **2004**, *108*, 17886−17892.
(14) Greeley, J.; Jaramillo, T. F.; Bonde, J.; Chorkendorff, I.; Nørskov, J. K. *Nat. Mater.* **2006**, *5*, 909−913.
(15) Greeley, J.; Nørskov, J. K. *J. Phys. Chem. C* **2009**, *113*, 4932−4939.
(16) Greeley, J.; Stephens, I.; Bondarenko, A.; Johansson, T.; Hansen, H. A.; Jaramillo, T.; Rossmeisl, J.; Chorkendorff, I.; Nørskov, J. K. *Nat. Chem.* **2009**, *1*, 552−556.
(17) Zambelli, T.; Wintterlin, J.; Trost, J.; Ertl, G. *Science* **1996**, *273*, 1688−1690.
(18) Haruta, M.; Daté, M. *Appl. Catal., A* **2001**, *222*, 427−437.
(19) Bratlie, K. M.; Lee, H.; Komvopoulos, K.; Yang, P.; Somorjai, G. A. *Nano Lett.* **2007**, *7*, 3097−3101.
(20) Williams, W. D.; Shekhar, M.; Lee, W.-S.; Kispersky, V.; Delgass, W. N.; Ribeiro, F. H.; Kim, S. M.; Stach, E. A.; Miller, J. T.; Allard, L. F. *J. Am. Chem. Soc.* **2010**, *132*, 14018−14020.
(21) Martinez, U.; Vilhelmsen, L. B.; Kristoffersen, H. H.; Stausholm-Møller, J.; Hammer, B. *Phys. Rev. B* **2011**, *84*, 205434.
(22) Liu, P.; Nørskov, J. K. *Phys. Chem. Chem. Phys.* **2001**, *3*, 3814−3818.
(23) Chen, M.; Kumar, D.; Yi, C.-W.; Goodman, D. W. *Science* **2005**, *310*, 291−293.
(24) Du, B.; Tong, Y. *J. Phys. Chem. B* **2005**, *109*, 17775−17780.
(25) Mallat, T.; Orglmeister, E.; Baiker, A. *Chem. Rev.* **2007**, *107*, 4863−4890.
(26) Laliberté, M.-A.; Lavoie, S.; Hammer, B.; Mahieu, G.; McBreen, P. H. *J. Am. Chem. Soc.* **2008**, *130*, 5386−5387.
(27) Demers-Carpentier, V.; McBreen, P. H. *J. Phys. Chem. C* **2011**, *115*, 6513−6520.
(28) Szőllősi, G.; Cserényi, S.; Bucsi, I.; Bartók, T.; Fülöp, F.; Bartók, M. *Appl. Catal., A* **2010**, *382*, 263−271.
(29) Balázsik, K.; Szőri, K.; Szőllösi, G.; Bartók, M. *Catal. Commun.* **2011**, *12*, 1410−1414.
(30) Brunelle, J.; Demers-Carpentier, V.; Lafleur-Lambert, R.; Mahieu, G.; Goubert, G.; Lavoie, S.; McBreen, P. H. *Top. Catal.* **2011**, *54*, 1334−1339.
(31) Demers-Carpentier, V.; Laliberté, M.-A.; Pan, Y.; Mahieu, G.; Lavoie, S.; Goubert, G.; Hammer, B.; McBreen, P. H. *J. Phys. Chem. C* **2011**, *115*, 1355−1360.
(32) Demers-Carpentier, V.; Goubert, G.; Masini, F.; Dong, Y.; Rasmussen, A. M. H.; Hammer, B.; McBreen, P. H. *J. Phys. Chem. Lett.* **2011**, 92−96.
(33) Bahn, S. R.; Jacobsen, K. W. *Comput. Sci. Eng.* **2002**, *4*, 56−66.
(34) Mortensen, J. J.; Hansen, L. B.; Jacobsen, K. W. *Phys. Rev. B* **2005**, *71*, 035109.
(35) Enkovaara, J.; Rostgaard, C.; Mortensen, J. J.; Chen, J.; Dułak, M.; Ferrighi, L.; Gavnholt, J.; Glinsvad, C.; Haikola, V.; Hansen, H. A.; Kristoffersen, H. H.; Kuisma, M.; Larsen, A. H.; Lehtovaara, L.; Ljungberg, M.; Lopez-Acevedo, O.; Moses, P. G.; Ojanen, J.; Olsen, T.; Petzold, V.; Romero, N. A.; Stausholm-Møller, J.; Strange, M.; Tritsaris, G. A.; Vanin, M.; Walter, M.; Hammer, B.; Häkkinen, H.; Madsen, G. K. H.; Nieminen, R. M.; Nørskov, J. K.; Puska, M.; Rantala, T. T.; Schiøtz, J.; Thygesen, K. S.; Jacobsen, K. W. *J. Phys.: Condens. Matter* **2010**, *22*, 253202.
(36) Klimeš, J.; Bowler, D. R.; Michaelides, A. *J. Phys.: Condens. Matter* **2010**, *22*, 022201.
(37) Liu, W.; Carrasco, J.; Santra, B.; Michaelides, A.; Scheffler, M.; Tkatchenko, A. *Phys. Rev. B* **2012**, *86*, 245405.
(38) Henkelman, G.; Uberuaga, B. P.; Jónsson, H. *J. Chem. Phys.* **2000**, *113*, 9901−9904.
(39) Govender, A.; Ferré, D. C.; Niemantsverdriet, J. W. H. *ChemPhysChem* **2012**, *13*, 1591−1596.
(40) Porezag, D.; Pederson, M. R. *Phys. Rev. B* **1996**, *54*, 7830−7836.
(41) Demers-Carpentier, V.; Goubert, G.; Masini, F.; Lafleur-Lambert, R.; Dong, Y.; Lavoie, S.; Mahieu, G.; Boukouvalas, J.; Gao, H.; Rasmussen, A. M. H.; Ferrighi, L.; Pan, Y.; Hammer, B.; McBreen, P. H. *Science* **2011**, *334*, 776−780.
(42) Goubert, G.; Rasmussen, A. M. H.; Dong, Y.; Groves, M. N.; McBreen, P. H. Hammer, B. *Surf. Sci.*, Submitted.
(43) Lin, S. D.; Sanders, D. K.; Vannice, M. A. *Appl. Catal., A* **1994**, *113*, 59−73.
(44) Sen, B.; Vannice, M. A. *J. Catal.* **1988**, *113*, 52−71.
(45) Busygin, I.; Taskinen, A.; Nieminen, V.; Toukoniitty, E.; Stillger, T.; Leino, R.; Murzin, D. Y. *J. Am. Chem. Soc.* **2009**, *131*, 4449−4462.
(46) Loffreda, D.; Delbecq, F.; Vigné, F.; Sautet, P. *Angew. Chem., Int. Ed.* **2005**, *44*, 5279−5282.
(47) Saeys, M.; Reyniers, M.-F.; Marin, G. B.; Neurock, M. *J. Phys. Chem. B* **2002**, *106*, 7489−7498.
(48) Watwe, R. M.; Cortright, R. D.; Mavrikakis, M.; Nørskov, J. K.; Dumesic, J. A. *J. Chem. Phys.* **2001**, *114*, 4663−4668.
(49) Morin, C.; Simon, D.; Sautet, P. *Surf. Sci.* **2006**, *600*, 1339−1350.

(50) Houle, F. A.; Beauchamp, J. L. *J. Am. Chem. Soc.* **1978**, *100*, 3290−3294.
(51) Eiden, G. C.; Lu, K.-T.; Badenhoop, J.; Weinhold, F.; Weisshaar, J. C. *J. Chem. Phys.* **1996**, *104*, 8886−8895.
(52) Rice, J. E.; Handy, N. C.; Knowles, P. J. *J. Chem. Soc., Faraday Trans. 2* **1987**, *83*, 1643−1649.
(53) Sinha, N. K.; Neurock, M. *J. Catal.* **2012**, *295*, 31−44.
(54) Loffreda, D.; Delbecq, F.; Vigné, F.; Sautet, P. *J. Am. Chem. Soc.* **2006**, *128*, 1316−1323.
(55) Saeys, M.; Reyniers, M.-F.; Neurock, M.; Marin, G. B. *J. Phys. Chem. B* **2003**, *107*, 3844−3855.
(56) Neurock, M.; van Santen, R. A. *J. Phys. Chem. B* **2000**, *104*, 11127−11145.
(57) Delbecq, F.; Loffreda, D.; Sautet, P. *J. Phys. Chem. Lett.* **2010**, *1*, 323−326.
(58) Demers-Carpentier, V.; Laliberté, M.-A.; Lavoie, S.; Mahieu, G.; McBreen, P. H. *J. Phys. Chem. C* **2010**, *114*, 7291−7298.
(59) Meemken, F.; Baiker, A.; Dupré, J.; Hungerbühler, K. *ACS Catal.* **2014**, *4*, 344−354.
(60) Gudmundsdóttir, S.; Skúlason, E.; Weststrate, K.-J.; Juurlink, L.; Jónsson, H. *Phys. Chem. Chem. Phys.* **2013**, *15*, 6323−6332.
(61) Gudmundsdóttir, S.; Skúlason, E.; Jónsson, H. *Phys. Rev. Lett.* **2012**, *108*, 156101.
(62) Cakl, Z.; Reimann, S.; Schmidt, E.; Moreno, A.; Mallat, T.; Baiker, A. *J. Catal.* **2011**, *280*, 104−115.
(63) Mallat, T.; Orglmeister, E.; Baiker, A. *Chem. Rev.* **2007**, *107*, 4863−4890.
(64) Mallat, T.; Bodmer, M.; Baiker, A. *Catal. Lett.* **1997**, *44*, 95−99.
(65) Varga, T.; Felföldi, K.; Forgó, P.; Bartók, M. *J. Mol. Catal. A: Chem.* **2004**, *216*, 181−187.
(66) Vargas, A.; Bürgi, T.; von Arx, M.; Hess, R.; Baiker, A. *J. Catal.* **2002**, *209*, 489−500.
(67) Hess, R.; Mallat, T.; Baiker, A. *J. Catal.* **2003**, *218*, 453−456.
(68) Murzin, D. Y.; Mäki-Arvela, P.; Toukoniitty, E.; Salmi, T. *Catal. Rev. Sci. Eng.* **2005**, *47*, 175−256.
(69) Hall, T.; Johnston, P.; Vermeer, W.; Watson, S.; Wells, P. In *Studies in Surface Science Catalysis*; Hightower, J., Delgass, W., Iglesia, E., Bell, A., Eds.; Elsevier: New York, 1996; Vol. *101*; pp 221−230.
(70) Lavoie, S.; Laliberté, M.-A.; Mahieu, G.; Demers-Carpentier, V.; McBreen, P. *J. Am. Chem. Soc.* **2007**, *129*, 11668−11669.
(71) Toukoniitty, E.; Mäki-Arvela, P.; Kuzma, M.; Villela, A.; Neyestanaki, A. K.; Salmi, T.; Sjöholm, R.; Leino, R.; Laine, E.; Murzin, D. Y. *J. Catal.* **2001**, *204*, 281−291.
(72) Toukoniitty, E.; Franceschini, S.; Vaccari, A.; Murzin, D. Y. *Appl. Catal., A* **2006**, *300*, 147−154.
(73) Nieminen, V.; Taskinen, A.; Hotokka, M.; Murzin, D. Y. *J. Catal.* **2007**, *245*, 228−236.
(74) Vargas, A.; Bürgi, T.; Baiker, A. *J. Catal.* **2004**, *222*, 439−449.